Valente, J.; Quintana-Solorzano, R.; Armendariz-Herrera, H.; Barragan-Rodriguez, G.; López Nieto, JM. (2014). Kinetic Study of Oxidative Dehydrogenation of Ethane over MoVTeNb Mixed-Oxide Catalyst. Industrial and Engineering Chemistry Research. 53(5):1775-1786. doi:10.1021/ie402447h.

Kinetic study of oxidative dehydrogenation of ethane over MoVTeNb mixed oxide catalyst

Jaime S. Valente[(a)], R. Quintana-Solórzano[(a)*], H. Armendáriz-Herrera[(a)], G. Barragán-Rodríguez[(a)], J. M. López-Nieto[(b)],*

[(a)]Instituto Mexicano del Petróleo, Eje Central Lázaro Cárdenas N°152, México, DF., C. P. 07730, Mexico

[(b)]Instituto de Tecnología Química, UPV-CSIC, Campus de la Universidad Politécnica de Valencia, Av. de los naranjos s/n, 46022 Valencia, Spain

[*]To whom correspondence should be addressed

Telephones: +52 55 9175 8444 (J.S.V.) and +52 55 9175 8530 (R.Q.S.)

e-mails: jsanchez@imp.mx(J.S.V.); rquintana@imp.mx(R.Q.S.)

Abstract

A MoVTeNb multimetallic mixed oxide was studied for the oxidative dehydrogenation (ODH) of ethane, a promising alternative for catalytic ethylene production. Lab-scale steady-state experimental reaction data, according to a 3^k experimental designto investigate the simultaneous effect of temperature (400-480 °C) and space-time [23–70 $g_{cat}h$ (mol ethane)$^{-1}$], were obtained. A fixed-bed reactor at atmospheric pressure was employed, feedingan ethane/oxygen/nitrogen mixture. Ethane conversion varies from 17 to 85%; whereas selectivity to ethylene and CO_x vary from 76 to 94%, and4.0 to 24 %, respectively. These types of analyses are useful for determining the optimum reactions conditions to enhance the catalytic performance of the mixed oxides herein presented.

Keywords: oxidative dehydrogenation; ethane; ethylene; MoVTeNb catalyst; kinetic modeling.

1 Introduction

Ethylene is the most important olefin in the petrochemical context, as it is the major raw material for the production of polymers. At present, commercial ethylene is obtained worldwide mainly from steam cracking of hydrocarbon cuts (*e.g.*, ethane, naphtha, gas oils, etc.), with a small contribution from the fluid catalytic cracking of gas oils (FCC process). Ethylene market follows an increase related to world population growth; hence, its demand is expected to increase continuously in the coming years.[1]

Currently, the main industrial process for ethylene production is steam cracking. This is a thermal conversion process, carried out at high temperatures (800 – 900 ^{o}C).[2] Hence, the associated energy demand is considerably large. Also, special metallurgy is required for the internal components of the furnace, and the high operation temperature increases the occurrence of side reaction. Thus, the global selectivity to ethylene is reduced, and a large diversity of by-products is obtained (e.g., acetylene, methane, propane, butane, etc.). The downstream separation scheme is therefore relatively complex.[3,4]

Catalytic dehydrogenation of ethane is also very demanding in energetic terms, due to the thermodynamic limitations associated to the endothermic nature of the reaction ($\Delta H^{o}_{R,298K}$= 135.9 kJ mol^{-1}; $\Delta G^{o}_{R,298K}$= 100.3 kJ mol^{-1}). The reaction must be performed above 700^{o}C to be commercially attractive.[5] Direct dehydrogenation of ethane has been improved with the incorporation of active and selective catalysts; however, these are susceptible to deactivation by coke (a high molecular mass side product inevitably formed in course of the reaction).[6]

Concerning the FCC process, it is aimed at producing gasoline, diesel as well as C_3-C_4 olefins; hence, ethylene is produced in relatively low amounts.

In view of the various disadvantages described above, combined with a worldwide interest on increasing ethylene production and the gradual increase in demand for petroleum-based products, it is urgent to develop new alternatives for ethylene production.[3-5] For several years now, oxidative dehydrogenation (ODH) of ethane has been an investigation subject of great interest. ODH of ethane is performed over a solid catalyst, wherein ethane reacts with oxidant species, typically oxygen.[5] Several advantages are noticed when comparing ethane ODH versus the existing commercial processes.[7] In the ethane ODH process: (*i*) no thermodynamic limitations exist ($\Delta G^{o}_{r,298K}$= -128 kJ mol^{-1}), (*ii*) the reaction is exothermic ($\Delta H^{o}_{r,298K}$= -106 kJ mol^{-1}),eliminating the need of an external heat supply, (*iii*) a limited number of reaction products areobserved (mainly CO_x, aside from ethylene) and (*iv*) no catalyst deactivation by coke is expected, owing to the oxygenpresent in the reaction medium. Commercial production of ethylene via ethane ODH remains a challenge.[2,5] The key lies in developing a catalyst with adequate properties: it should be able to transform ethane at low temperatures, and produce ethylene while minimizing CO_x formation. It has been reported that an attractive scenario for ethane ODH would present ethylene selectivity larger than 90% and ethane conversion greater than 60%, at temperatures lower than 500 °C.[2,3] High selectivity to ethylene is one of the most important features of a suitable catalyst, not only for economic feasibility, but also because the combustion reactions responsible for the formation of CO and CO_2 are *ca.*8 and 13 times more exothermic, respectively, than ethylene production from ethane. This would represent an important issue for operational reactor control, due to the hot points generated by the aforementioned combustion reactions. Aimed at fulfilling both activity and selectivity requirements, a large variety of catalytic systems have been proposed.[4-6,8] Thus far, one of the most efficient and promising catalysts for partial oxidations reactions, particularly for ethane

ODH, is amultimetallic mixed oxide that contains Mo, Te, V and Nb, which has been described and studied by several research groups.[9-14]

MoTeVNb-based materials consist of a mixture of crystalline phases, mainly two, denoted in scientific literature as M1 and M2.[9-18] M1 phase has been shown to be the responsible of the activity, as it holds the active and selective surface sites needed for partial oxidation of ethane.[10-14,18-20] The activation of this catalytic formulation occurs at around 350 °C, exhibiting acceptable values of ethane conversion with a remarkably high selectivity to ethylene. Even though some information concerning the effect of temperature and other important operating conditions on the performance of these catalysts for ethane ODH have been reported in literature.[5,10-14,18-20] To the best of our knowledge no reports have been published for the MoTeVNb mixed oxide catalytic system, in particular, correlating kinetic aspects with temperature, space-time and ethane and oxygen inlet partial pressure.

Where kinetic models are concerned, few models have been proposed to describe ethane ODH over different types of catalytic systems by applying Power-Law, Langmuir-Hinshelwood, Eley-Rideal, and Mars and van Krevelen formalisms.[23-29] Kinetic models are specific for a given catalytic formulation; hence, available published information related to kinetic parameters (*i.e.*, activation energies, pre-exponential factors) as well as adsorption parameters is diverse.

The aim of this work is to elucidate the effect of temperature, space-time, and ethane and oxygen inlet partial pressure on the steady-state catalytic performance of MoVTeNb multimetallic mixed oxide for ethane ODH to ethylene. The effects of temperature and space-time, two of the most important variables in the operation of catalytic reactors, were assessed by applying a 3^k experimental design. A statistical analysis of the experimental design is carried out to determine the significance of main factors effects and their interaction on a set of selected catalytic responses. 3D surface plots are next used to explore convenient operation regions for

some representative catalytic responses, such as ethane conversion, ethylene selectivity, CO_x selectivity and space time yield (STY) of ethylene.Therefore, a power-law based kinetic model was developed by varying: reaction temperature from 400 to 480 °C, space-time($w_{cat}F^{-1}_{ethane,o}$) from 10 to 140 g_{cat} h(mol fed ethane)$^{-1}$, and ethane and oxygen inlet partial pressure, from 5.1 to 22.3 kPa. Although power-law based kinetics disregard mechanistic aspects, they are extensively used for reactor scaling-up and design.

2 Experimental and procedures

2.1 Catalysts preparation

A MoVTeNb multimetallic mixed oxide with Mo:V:Te:Nb=1:0.24:0.24:0.18 nominal atomic ratios, was prepared. Briefly, the synthesis of the catalyst involved the following steps: (*i*) an aqueous solution containing tetra-hydrated ammonium heptamolybdate (MERK, 99%), telluric acid (Aldrich, 98 %) and ammonium metavanadate (Sigma-Aldrich, 99.5%) was prepared under continuous stirring,at 80 °C; (*ii*) separately, an aqueous solution of niobium oxalate (ABCR laboratories, 99%) and oxalic acid (Aldrich, 98%) was prepared, also at 80 °C. Solution (*ii*) was added to the solution of step (*i*) maintaining a vigorous continuous stirring. The resulting mixturetransformed into slurry, which was cooled down to room temperature. Then, the pH of the slurry was adjusted to 2.5 by adding 1 M nitric acid solution. The acidified slurry was subsequently placed in a rotavapor system,in order to gradually evaporate water at 50 °C and 27 kPa. The resulting powder was dried overnight at 100 °C and lastly thermally treated 600 °C for 2 h under nitrogen flow.

2.2 Catalyst characterization

The catalyst was characterized by X-ray power diffraction technique, in a Siemens D-500 diffractometer provided with a θ-θ configuration and a graphite secondary-beam monochrome. Diffraction was measured from 4 to 80° with a 2θ step of 0.02° for 8 s per point, using $CuK\alpha_{1,2}$ radiation with a wavelength of 1.5418 as well as a power of 40 kV and 40 Ma.

Solid´s chemical composition was determined in a Perkin Elmer Mod. OPTIMA 3200 Dual Vision by inductively coupled plasma atomic emission spectrometry (ICP-AES).

The specific surface area of the calcined powdered catalyst was analyzed by N_2 physisorption at -196 ºC on an AUTOSORB-I apparatus. Prior to the analysis, the sample was outgassed in a vacuum (10^{-5}Torr) at 300 °C for 5 h. The specific surface areawas calculated by using the Brunauer-Emmett-Teller (BET) method.

2.3 Catalytic testing

2.3.1 Reactor and chromatographic set-up

The catalytic experiments were performed in a semi-automatized lab-scale set-up, equipped with a 10 mm internal diameter/40 mm length fixed-bed quartz tubular reactor, operated isothermally, at atmospheric pressure and integral regime. The reactor is provided with two thermocouples, one indicating the reactor wall temperature and the other measuring the catalyst bedtemperature. All runs were performed feeding the reactor with a mixture consisting of ethane (C_2) and oxygen (O_2), as well as nitrogen (N_2) as diluent. The N_2 was also employed as internal standard. The purity of ethane, oxygen and nitrogen utilized in the experiments were 99.7 vol%, 99.996 vol% and 99.999 vol%, respectively. The flow rate of the gases was quantified using independent thermal Mass Flow Controllers (MFC) Brooks 5850I.

The reactor effluent was analyzed periodically on-line by gas chromatography (GC). Said analysis was conducted in a HP-7890 series II GC equipped with FID and TCD detectors, with an array of three columns: a 30 m×530 μm×50 μm HP Plot Q capillary, a 30 m×530 μm× 40 μm molecular sieve and a 30 m× 0.25 mm ×5 μm HP Plot alumina. Although hydrocarbons are observable in both TCD and FID, they were quantified in the FID owing to its higher sensitivity to these compounds. The other reaction products, i.e., CO_2 and CO, as well as oxygen and nitrogen, were identified in the TCD.

2.3.2 Operating conditions

For a typical experiment, 0.60 g of thermally treated catalyst with average size particles of 150 μm was loaded into the reactor. Before reaction testing, the gaseous mixture composition was verified byGC, it was preheated at 140 °C. The reactor was heated with a furnace and set to the intended temperature. A blank experiment, carried out at 480 °C, confirmed the absence of both ethane and oxygen conversions in the absence of catalyst. The reaction was followed for six hours. In all experiments, carbon balance reported values within the range 100±2.0 %.

For a systematic investigation of the concomitantinfluence of temperature and space-time on the catalytic behavior of the MoVTeNb, a first set of experiments were performed in accordance with a factorial experimental design. Here, inlet partial pressures of ethane, oxygen and nitrogen were fixedat 7.0, 5.5 and 65.5 kPa, respectively. Since a non-linear effect of temperature over some responses is expected and considering that only two independent factorswill be studied, a 3^k design was proposed, k being the number of independent factors and "3"denoting the number of levels of the factors explored. The specific levels of the factors, temperature and space-time in this case, are denoted as low (0), medium (1) and high (2) for the lowest, intermediate and highest values of the factor. Specifically, temperature was varied from 400–480 °C and space-time between 23 and 70 $g_{cat}h$ (mol fed ethane)$^{-1}$. The number of

combinations between factors and corresponding levels gives 9 (3^2) denoting the number of independent experiments to be performed for a genuine replicate (n). Aimed at calculating the error of the experimental design, two genuine replicates, n=2, were accounted for. Independent variables, other than temperature and space-time, were kept at the values outlined in section 2.3.2.The maximum operation temperature was set to 480 °C.Even though several catalytic responses (*e.g.* conversion, selectivity, yield, etc.)could be considered in the experimental design, only four responses were taken into account (*vide infra*).

In a second set of experimentscarried out at 440 °C, inlet partial pressure of ethane ($P^o_{C_2}$) was varied at constant inlet partial pressure of oxygen ($P^o_{O_2}$) and viceversa. To obtain values of overall rates, space-time was also changed in this set. Inlet partial pressures of ethaneand oxygen wereranged from 5.1 to 22.3 kPa, whereas space-time was varied from 10–140 $g_{cat}h$(mol fed ethane)$^{-1}$. At these operating conditions, the ratio ethane to oxygen in the feed varies from 0.5 to 2.0.

An assessment of transport limitations for the main reaction was performed in accordance to the different criteria reported in literature.[30,31] Concentration and temperature gradients were found to be below suggested limits,[31] while criteria for plug-flow mode and isobaric operation at the reactor bed scale were also fulfilled.

2.3.3 Calculations of the value of responses considered in the experimental design

The factors selected in the experimental design were ethane conversion, ethylene selectivity and space time yield (STY) of ethylene. Ethane conversion and ethylene selectivity were defined on a carbon basis. Ethane conversion was calculated by equation 1

$$X_{C,ethane}=\frac{G^o_{C,ethane}-G_{C,ethane}}{G^o_{C,ethane}}\times 100 \quad (1)$$

where, $G^{o}_{C,ethane}$ and $G_{C,ethane}$ denote the mass flow of ethane at the inlet and outlet of the reactor, respectively.

Selectivity to ethylene and oxidation products, CO and CO_2, were computed considering the carbon mass in component *i* formed per mass of carbon in ethane converted according to equation 2.

$$S_{C,i}=\frac{G_{C,i}}{G^{o}_{C,ethane}-G_{C,ethane}}\times 100 \quad (2)$$

The ethane flow at the reactor entrance was quantified by the MFC, measured at standard conditions, *i.e.*, 1 atm (101.32 kPa) and 20 °C. The flow at the reactor outlet was quantified via the internal standard method according to equation 3.

$$F_i=\frac{F^{o}_{N2}M_{N2}}{A_{N2}Cf_{N2}}\times\frac{A_iCf_i}{M_i} \quad (3)$$

where, Fi is the outlet molar flow rate of compound *i*, calculated from molecular mass (M), GC-integrated area (A) and GC-calibration factor (Cf) of product *i*; the corresponding values of nitrogen were used as internal standard (F^{o}_{N2} is the molar flow rate).

The carbon flow in compound *I*, at the reactor outlet, is calculated by considering the number of carbons in the molecule as well as carbon's atomic mass, by equation 4.

$$G_{C,i}=12\times F_i\times C_{atoms,i} \quad (4)$$

The third factor, accounting for STY of ethylene, is defined as the grams of ethylene produced per hour and per kilogram of catalyst. It is calculated by means of equation 5.

$$STY=\frac{F_{ethylene}M_{ethylene}}{W_{cat}} \quad (5)$$

2.4 Kinetic modeling

2.4.1 Reaction network and rate expressions

The reaction network employed for the kinetic modeling of ethane ODH is presented in Scheme1.

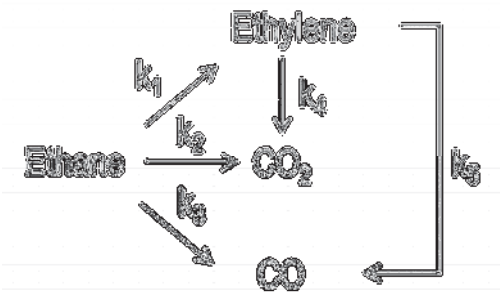

Scheme 1. Reaction network employed for the kinetic modeling of ethane ODH.

In accordance with this scheme, ethane reacts with oxygen to produce ethylene, CO_2 as well as CO. Produced ethylene is susceptible to subsequent reactions, converting it into CO_2 and/or CO. The reaction rates are described by power law rate equations; hence, a rate coefficient is included, as are the partial pressure of reagents (ethane, ethylene and oxygen), and reaction orders for each reagent. For the species involved in the network, their overall rates are expressed by the equations 6 to 9.

$$R_{ethane} = -(k_1 P_{ethane}^{\alpha 1} P_{oxygen}^{\beta 1} + k_2 P_{ethane}^{\alpha 2} P_{oxygen}^{\beta 2} + k_3 P_{ethane}^{\alpha 3} P_{oxygen}^{\beta 3}) \quad (6)$$

$$R_{ethylene} = k_1 P_{ethane}^{\alpha 1} P_{oxygen}^{\beta 1} - k_4 P_{ethylene}^{\alpha 4} P_{oxygen}^{\beta 4} - k_5 P_{ethylene}^{\alpha 5} P_{oxygen}^{\beta 5} \quad (7)$$

$$R_{CO2} = 2.0(k_2 P_{ethane}^{\alpha 2} P_{oxygen}^{\beta 2} + k_4 P_{ethylene}^{\alpha 4} P_{oxygen}^{\beta 4}) \quad (8)$$

$$R_{CO} = 2.0(k_3 P_{ethane}^{\alpha 3} P_{oxygen}^{\beta 3} + k_4 P_{ethylene}^{\alpha 5} P_{oxygen}^{\beta 5}) \quad (9)$$

where, α_1, $\alpha 2$,…, α_5 are the reaction orders related to the partial pressure of hydrocarbon (ethane or ethylene), while β_1, …, β_5 denote the reaction orders associated to the partial pressure of oxygen, which must be determined experimentally.

For oxygen and water, which were not explicitly included in the network of Scheme 1, the corresponding overall rates are given by the equations 10 and 11.

$$R_{O2} = -0.5k_1 P_{ethane}^{\alpha 1} P_{oxygen}^{\beta 1} - 3.5k_2 P_{ethane}^{\alpha 2} P_{oxygen}^{\beta 2} - 2.5k_3 P_{ethane}^{\alpha 3} P_{oxygen}^{\beta 3}$$

$$- 3.0(k_4 P_{ethylene}^{\alpha 4} P_{oxygen}^{\beta 4} - k_5 P_{ethylene}^{\alpha 5} P_{oxygen}^{\beta 5}) \quad (10)$$

$$R_{H2O} = k_1 P_{ethane}^{\alpha 1} P_{oxygen}^{\beta 1} + 3.0(k_2 P_{ethane}^{\alpha 2} P_{oxygen}^{\beta 2} + k_3 P_{ethane}^{\alpha 3} P_{oxygen}^{\beta 3})$$

$$+ 2.0(k_4 P_{ethylene}^{\alpha 4} P_{oxygen}^{\beta 4} + k_5 P_{ethylene}^{\alpha 5} P_{oxygen}^{\beta 5}) \quad (11)$$

The constants k_i used in equations 6 to 11 are the rate coefficients (i = 1, 2,…, 5) denoting the reaction according to the assigned number in Scheme 1. They are temperature-dependent, calculated in accordance with the Arrhenius expression of equation 12.

$$k_i = A_i \exp^{(\frac{-Ei}{RT})} \quad (12)$$

where, E_i is the activation energy and A_i is the pre-exponential factor of i. The determination of E_i and A_i, with corresponding statistics, is accomplished using experimental data at different temperatures.

In order to reduce the initial correlation of pre-exponential factors with activation energies, the pre-exponential factors were used in the reparameterized form. Consequently, the rate coefficient of a reaction i was computed according to the reparameterized Arrhenius expression by the equation 13

$$k_i = A_{rep,i} \exp\left(\frac{E_i}{R}\left[\frac{1}{T_m} - \frac{1}{T}\right]\right) \quad (13)$$

The reparameterized pre-exponential factor designated $A_{rep,i}$ is calculated by using the equation 14.

$$A_{rep,i} = A_i \exp(-\frac{E_i}{RT_m}) \quad (14)$$

where, T_m is the mean temperature.

2.4.2 Reactor model equations and parameters estimation

Parameter estimation was performed by minimizing the weighted sum of squares of the residuals (RSS) between kinetic model predicted yields, referred to as $\hat{Y}_{i,j}$, and experimental molar yields, designated Y_{ij}, for the species of the reaction network of Scheme1, according to equation 15.

$$RSS(\beta)= \sum_{i=1}^{nobs} \sum_{j=1}^{nresp} w_j (Y_{i,j}-\hat{Y}_{i,j})^2 \xrightarrow{\beta_1,\ \beta_2,\ \dots\ \beta_{np}} \min \quad (15)$$

where, β is the vector of kinetic parameters estimated via regression, n_{obs} is the number of independent experiments, n_{resp} is the number of responses, n_p is the number of parameters, and w_j is a weight factor that can be optionally used for tuning the relative importance of the various responses. For an experiment i, the experimental molar yield of a species j was calculated by the equation 16.

$$Y_{i,j}=\frac{F_{i,j}}{F^{o}_{i,ethane}}\times 100 \quad (16)$$

Predicted yields considered in the objective function, were obtained according to equation 17, via numerical integration of the corresponding reactor model equations, given in a set of ordinary differential equations (ODEs).

$$R_{i,j}= \frac{d\hat{Y}_{i,j}}{d(w_{cat}F^{-1}_{ethane,o})_i} \quad (17)$$

With $Y_{i,j}(0)=0.0$ as boundary condition for experiment i and species j. For the i-th experiment, the overall rate formation of species j represented by $R_{i,j}$ is given by equations 6 to 11.

Equation 17 describes a continuous pseudo-homogeneous, isothermal, isobaric 1D plug flow reactor, operated in the integral regime, in the absence of concentration and thermal

gradients. Numerical integration of the ODEs given by equation 17 was carried out by using LSODA routine.[32]

ODRPACK 2.01 solver[33] was used to obtain the parameters that minimize the objective function (vide eq. 14) by nonlinear ordinary least squares for explicit models, with an implementation of the Levenberg-Marquardt method. In a first stage, rate coefficients were estimated at each temperature in order to obtain initial values for activation energies and pre-exponential factors using Arrhenius-type plots. In a second stage, the temperature dependence of the parameters was calculated by using the experimental data at all temperatures and estimating directly the values of activation energies and reparameterized pre-exponential factors. In order to assess the parameter estimation results, the F-test for the global significance of the regression and the individual confidence intervals based on the t-test for the estimates were computed.

2.4.3 Apparent reaction orders

In the case of multi-reaction system, contrary to what occurs in a single reaction case, the reaction orders associated to each reaction are not directly accessible from experimental data. Instead, kinetic orders for the various reactants can be determined from the corresponding overall reactions considering they can also expressed in terms of a power law kinetic formalism, as expressed by equation 18 for a species j:

$$R_j = \sum_{i=1}^{nr} k_i P_{ethane}^{\alpha i} P_{O2}^{\beta i} = k_j \; P_{ethane}^{mj} P_{O2}^{nj} \qquad (18)$$

The overall rate of species j takes into consideration the contribution of all the reactions, i=1, 2, …, n_r. Kinetic orders for species are now n_j and m_j, the former associated to the partial pressure of ethane and the later to the partial pressure of oxygen.

Thus, kinetic orders, related to ethane, are calculated from experiments varying P^{o}_{ethane} at a given value of P^{o}_{O2}; reaction orders of oxygen are computed via experiments modifying P^{o}_{O2} maintaining constant the value of P^{o}_{ethane}. Taking the natural logarithm of both sides of equation 18 and varying, for instance, only the inlet partial pressure of oxygen results in the equation 19.

$$\ln(R_j) = \text{constant} + n_j \ln(P_{O2}) \quad (19)$$

Experimental kinetic orders related to ethane and oxygen for a given product were then determined by applying the initial rates method.[33,34] Equation 17 is a continuity equation, a valid reaction model for a plug flow in the integral regime and in the absence of temperature and concentration gradients. Rate values are obtained from the first derivative of a space-time function expressed by the general form: $Y = f(w_{cat} F^{-1}_{ethane,o})$. Initial rates are then obtained by evaluating the first derivative of Y at space-time equal to zero. Subsequently, fitting $\ln(R^{o}_{j})$ and $\ln(P^{o}_{O2})$ data to a straight line gives a slope that corresponds to the n_j reaction order. Similar treatment is applied on $\ln(R^{o}_{j})$ and $\ln(P^{o}_{ethane})$ data to obtain the value of m_j kinetic order, associated to the partial pressure of ethane.

3 Results and discussion

3.1 Characterization of the MoVTeNb mixed oxide catalyst

The main physicochemical properties of the thermally activated MoVTeNb mixed oxide catalyst used for the kinetic study, are reported in supporting information. The specific surface area and the chemical composition of this material are comparable to those reported elsewhere for this type of solids.[13,35]

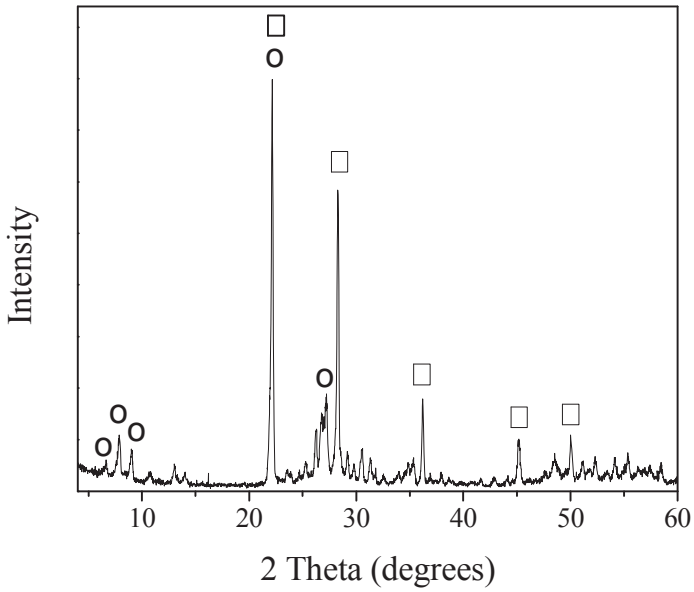

Figure 1. X-Ray diffraction pattern of the thermally activated MoVTeNb mixed oxide catalyst. (O) M1 phase and (□) M2 phase.

Regarding the crystalline phase composition calculated by Rietveld refinement, performed on X-ray diffraction pattern shown in Figure 1, the predominant M1 phase is observed (92 wt.%), to which the activity of this type of materials is attributed.[10-14,18-20] Indeed, this material presents an outstanding catalytic performance, as shall be demonstrated below.

3.2 Catalytic testing

During the catalyticexperiments,a limited number of reaction products (ethylene, CO and CO_2) were detected. Figure 2 shows the time-on-stream evolution of ethane and oxygen conversion as well as ethylene selectivity for an experiment performed at 440 °C and 35 g_{cat} h(mol fed ethane)$^{-1}$. A remarkable catalytic stability is observed, as no significant changes in conversion and selectivity were detected during the six-hour reaction test. In this experiment, the

catalyst exhibited a steady-state conversion of ethane as high as 48%, while that of oxygen reached a value of around 36%. In addition, high ethylene selectivity,*ca.* 93%, was attained.

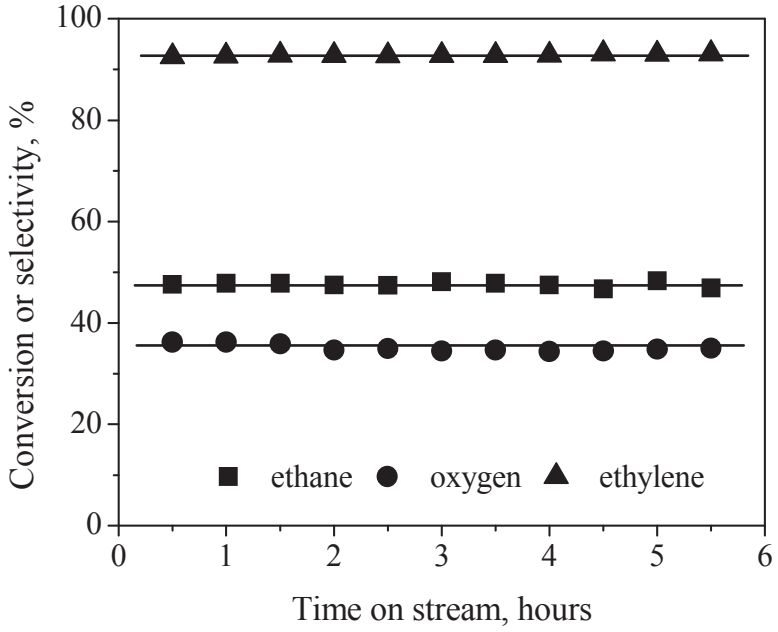

Figure 2. Ethane and oxygen conversions and ethylene selectivity. $T_{reaction}$= 440 °C, space-time = 35 g_{cat} h (mol ethane)$^{-1}$and inlet molar ratio $C_2/O_2/N_2$= 9/7/84.

Qualitatively, the effluent composition is in the following order: ethylene >> CO > CO_2. The relative amounts of these compounds vary as a function of both temperature and space-time; ethylene was the main product while the formation of CO was always higher than that of CO_2. Experiment results performed at 400–480 °C, 23-70 g_{cat} h (mol ethane)$^{-1}$ and an inlet molar ratio $C_2/O_2/N_2$= 9/7/84 show that ethane conversion ranged from 17 to 85 % and that of oxygen from 17 to 96 %. Concerning products distribution, as shown in Figure 3, selectivity to ethylene, CO and CO_2 varied from 76 to 94%, 2.5 to 17% and 1.5 to 7.5%, respectively. Additionally, the STY of ethylene values, a key parameter of interest for the petrochemical industry, changed from 122 to 640 $g_{ethylene}(kg_{cat}h)^{-1}$. Figure 3 displays the evolution of selectivity to ethylene, CO_2 and CO as

a function of ethane conversion. It is observed that, as the reaction conditions increase in severity, in terms of temperature and space-time, ethane conversion and CO_x selectivity grow, in detriment of selectivity to ethylene.

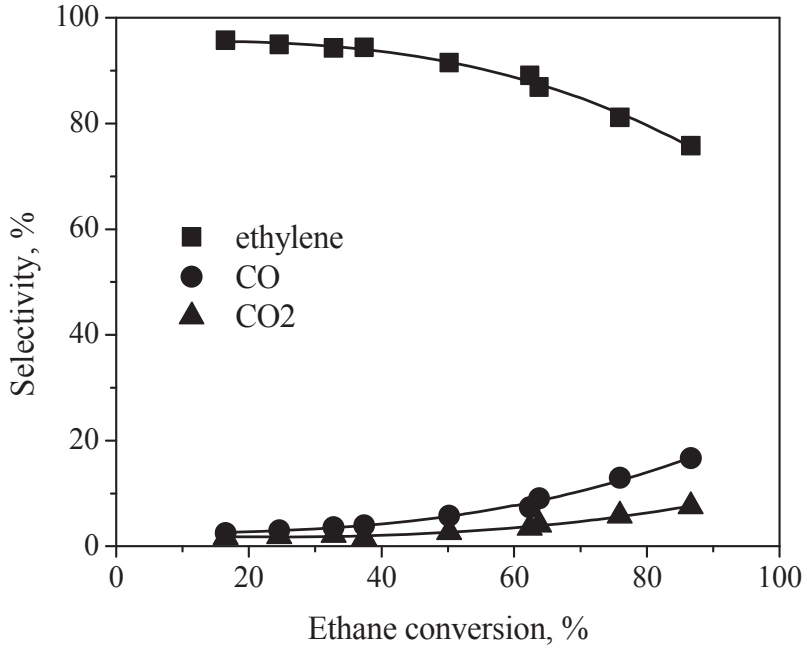

Figure 3. Variation of selectivity to ethylene, CO_2 and CO *versus* ethane conversion. $T_{reaction}$=400 – 480 °C, space-time = 23 to 70 g_{cat} h (mol ethane)$^{-1}$ and inlet molar ratio $C_2/O_2/N_2$ = 9/7/84.

3.3 Experimental design results

3.3.1 Main effects and interactions

As outlined previously, temperature (T) and space-time ($W_{cat}F^{-1}_{ethane,o}$, represented here as W), two key variables in the performance of catalytic reactors, were systematically studied by using reaction data generated in accordance with the 3^k factorial experimental design. For the sake of brevity, a selected group of responses was considered; in particular, ethane conversion, ethylene selectivity, CO_x selectivity as well as space time yield of ethylene (STY). Since similar trends were observed for CO and CO_2, they were grouped into CO_x.

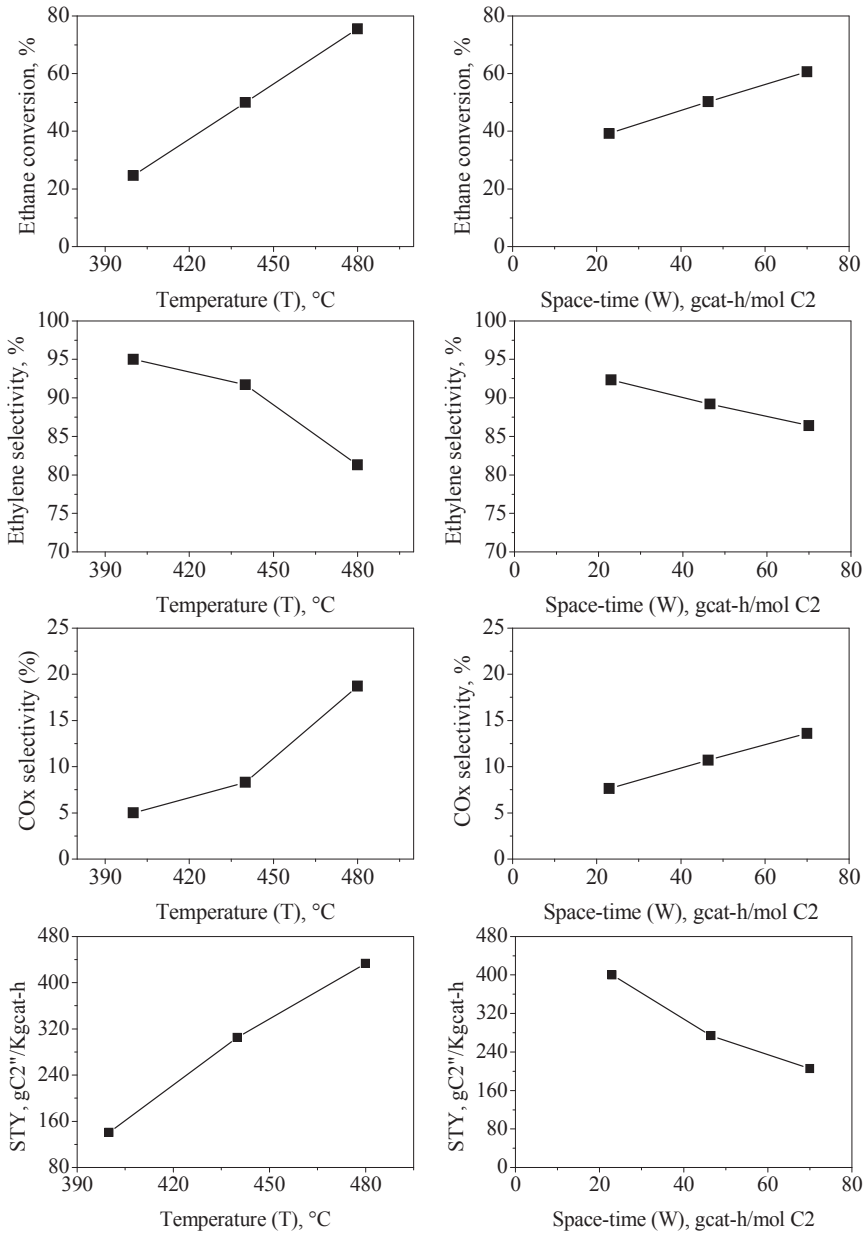

Figure 4. Main effects plot for ethane conversion, ethylene selectivity, CO_x selectivity and STY. From a 3^k factorial experimental design, varying temperature from 400 to 480 °C , space-time between 23 and 70 g_{cat} h (mol ethane)$^{-1}$and aninlet molar ratio $C_2/O_2/N_2$ = 9/7/84.

A goal of an experimental design is to detect the most important factors the extent of their influence for the considered responses. For a significant factor it is then necessary to identify the

nature of its impact on the response and, further, to determine the interaction of this factor with others considered in the design.[36-38] Figure 4 contains a set of graphs exhibiting the main effects for the four responses of interest. They are useful to visualize how the value of a response changes as a consequence of a continuous increase in the level of a given factor. Clearly, for ethane conversion and CO_x selectivity, increasing the level of both temperature and space-time has a positive effect on the response. Selectivity to ethylene is, in contrast, negatively affected by both temperature and space-time. The effect of temperature and space-time on STY has a different sign, *i.e.*, positive for the former and negative for the latter. On the basis of the slope of the main effect curves, it is deduced that the various responses are not equally affected by the changes in the level of temperature and space-time. It is noted that temperature has a strong effect on ethane conversion and STY, while space-time weakly affects ethylene selectivity.

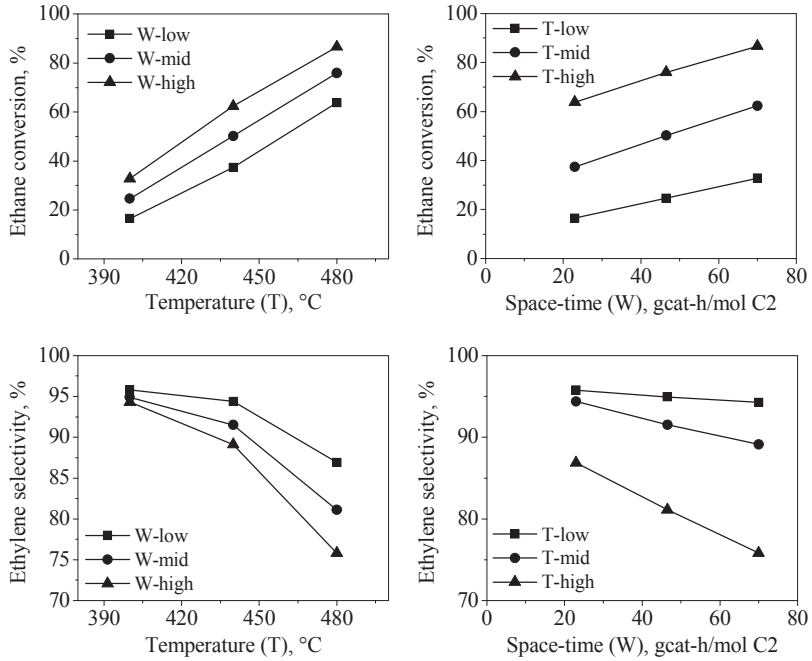

Figure 5. Interaction plots for the responses ethane conversion and ethylene selectivity. From a 3^k factorial experimental design, varying temperature from 400 to 480 °C , space-time between 23 and 70 g_{cat} h (mol ethane)$^{-1}$ and an inlet molar ratio $C_2/O_2/N_2$ = 9/7/84.

When differences between average responses associated to one factor vary as a function of the level of other factors, this indicates that an interaction between factors occurs.[39,40] Figures 4 and 5 contains the interaction plots for the studied responses. In the plots of conversion *vs.* temperature, and ethane conversion *vs.* space-time (Figure 5), the three lines in each graph are parallel, corresponding to a case in which no interaction between the two factors occurs. The other interaction plots in Figure 5, for ethylene selectivity; and Figure 6 for CO_x selectivity and STY of ethylene, contrast with those of ethane conversion. The three lines in each graph are not parallel, evidencing that there is an interaction between temperature and space-time in the case of these three responses.

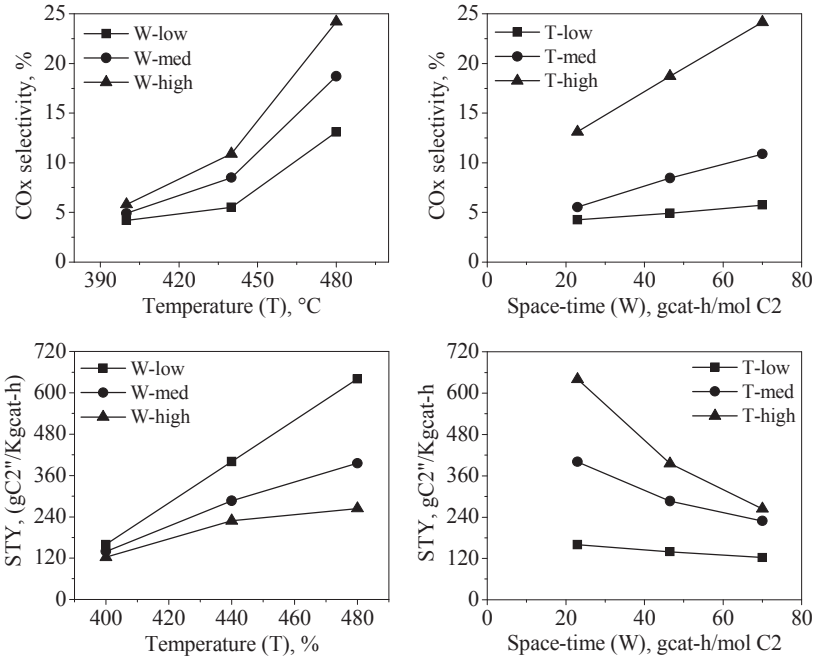

Figure 6. Interaction plots for the responsesCO_x selectivity and STY. From a 3^k factorial experimental design, varying temperature from 400 to 480 °C , space-time between 23 and 70 g_{cat} h (mol ethane)$^{-1}$ and an inlet molar ratio $C_2/O_2/N_2$ = 9/7/84.

On the basis of the interaction plots, the conclusive statements for the four responses analyzed are formulated in the following form: (*i*) for ethane conversion, the effect of

temperature and space-time is additive and, (*ii*) for ethylene selectivity, CO_x selectivity and STY of ethylene, the effect of space-time is non-additive and depends on temperature. Specifically, selectivity to ethylene is negatively affected by space-time and the value of this response decreases drastically as temperature increases, vide Figure 5. In the temperature range studied, STY of ethylene decreases with space-time, however, at low reaction temperature (400 °C) the STY of ethylene decline is slight, from 160 to 122 $g_{ethylene}(kg_{cat}\ h)^{-1}$,when space-time rises from 23 to 70 g_{cat} h (mol ethane)$^{-1}$. By contrast, at the high reaction temperature (480 °C), such a decrease is very pronounced from 640 to 264 $g_{ethylene}(kg_{cat}h)^{-1}$, vide Figure 6.

3.3.2 ANOVA analysis

A more detailed inspection of both main effects and interactions is needed to define which effects and interactions are statistically significant and to what extent for a given response, to this end, performing a variance analysis (ANOVA) is recommended.[37,38] The results of the ANOVA analysis for ethane conversion are shown in Table 1. ANOVA results for ethylene selectivity, CO_x selectivity and STY of ethylene are presented in supporting information. In these results, the main effects are separated into linear (L) and quadratic (Q), whereas global binary interactions are also decomposed to linear-linear (L-L), linear-quadratic, quadratic-linear (L-Q or Q-L), and quadratic-quadratic (Q-Q). Higher order interactions are usually negligible.[38] SS and MSS denote the sum of squares and medium squares, respectively, for the diverse sources of variation. F_o is the ratio of MSS of the variation source relative to that of the error. A comparison of F_o value with critical F-significance value test, in the form $F_{(1\text{-alpha},\ \upsilon 1,\upsilon 2)}$, allowed to determine whether a given source of variation is significant or not. Alpha is the probability level (95 % in all cases), υ_1 denotes the degrees of freedom (DF) of the source of variation and υ_2 the DF of the error. The

values of $F_{(1\text{-alpha},\, \upsilon 1,\upsilon 2)}$, also apply for the ANOVA results included in supporting information for the corresponding sources of variation.

Table 1. ANOVA results for ethane conversion (%).

Source of variation	SS	DF	MSS	F_o	F critical at 95%
W	2057.6	2	1028.8	2052.4	3.55
W_L	2057.0	1	2056.9	4103.6	4.41
W_Q	0.68	1	0.67	1.35	4.41
T	11623.7	2	5811.8	11594.5	3.55
T_L	11623.7	1	11623.7	23189.0	4.41
T_Q	0.02	1	0.02	0.04	4.41
T-W interactions	61.6	4	15.4	30.7	2.93
W_L -T_L	46.9	1	46.9	93.6	4.41
W_L-T_Q	14.4	1	14.4	28.7	4.41
W_Q-T_L	0.31	1	0.31	0.62	4.41
W_Q-T_Q	0.0011	1	0.001	0.002	4.41
Error	9.0	18	0.501	1.00	-
Total	13752.1	26	528.9	1055.2	-

SS, MSS and DF denote sum of squares, medium sum of squares and degrees of freedom, respectively; T represents temperature and W stands for space-time ($W_{cat}F^{-1}_{ethane,o}$).

Specific information obtained from the ANOVA analysis for ethane conversion is shown in Table 1. There, it is observed that the Q effect of both space-time (W) and temperature (T) is not significant; even though interaction W_L-T_L is significant at the 95% probability, its F_o value is relatively low suggesting a marginal influence on the response.

In the case of the selectivities to ethylene and CO_x presented in supporting information, the Q effect of space-time influences significantly the response's values, contrary to what occurs with W_Q. In the case of STY of ethylene shown in supporting information, both W_Q and T_Q

effects appear to be statistically significant, albeit the former exhibits a slightly larger value of F_o, compared to the critical F value.

From the analysis of ANOVA results of the four studied responses, it is generally noted that W_L and T_L effects have the largest influence among the variation sources. The W_L-T_L interaction is significant; conversely, the W_Q-T_L and W_Q-T_Q type interactions are not significant at the 95% level of probability. Also, it is observed that the F_o value of interaction W_L-T_Q is relatively low indicating a little influence of this interaction on the considered responses.

3.3.3 Regression analysis and surface responses

The next step in the analysis of the experimental design information is the proposal of a mathematical model, which is of great utility for prediction purposes. It correlates the value of a given response with the factors involved. Such models could be utilized for optimization purposes, *i.e.*, as a tool to estimate the values of the factors responses that maximize (or minimize) a specific response.[37]

In this work, a multiple non-linear regression analysis of the catalytic responses, obtained from experimental design data, was carried out to build models. Said analysis allows predicting the value of the responses for combinations of temperature and space-time within the experimental design region. For the sake of brevity, particular examples are offered for ethane conversion, ethylene selectivity and STY of ethylene as responses. On the basis of a previous assessment of main effects and interactions of factors via a variance analysis (ANOVA), a second order polynomia with the general form, represented by equation 20, was found to be suitable and general enough to represent the relation between a dependent variable or responses ($\widehat{Y}$) and independent variables (x_i).

$$\widehat{Y}=a_o+\sum_{i=1}^{k} a_i x_i+\sum_{i=1}^{k} a_{ii} x_i^2+\sum_i \sum_j a_{ij} x_i x_j \qquad (20)$$

Values of a_1, a_2, a_{11}, …, are closely linked with linear effects (a_i), quadratic effects (a_{ii}) and interactions (a_{ij}) between factors. Hence, equation 20 may be simplified when there exists evidence that effects and/or interactions are not statistically significant for a given response.

Equation 20, for instance, takes the form of equation 21, for predicting the value of response $\hat{y}$ as a function of temperature (T) and space-time (W) with a_0, a_1, a_2, a_{11}, etc., as parameters to be estimated via regression from the experimental design data.

$$\hat{Y}=a_o+a_1T+a_2W \quad +a_{11}T^2 \quad +a_{12}T\,W \quad +a_{22}W^2 \tag{21}$$

Table 2. Statistically significant main parameters values with 95 % confidence intervals related to the equation 21 proposed to fit ethane conversion, ethylene selectivity, COx selectivity and STY of ethylene.

Parameter	Response			
	Ethane conversion, %	Ethylene selectivity, %	COx selectivity, %	STY, $g_{ethylene}(h\ kg_{cat})^{-1}$
a_0	$(-2.51 \pm 0.094)\times10^{2}$	$(-3.08 \pm 0.33)\times10^{-1}$	$(-4.06 \pm 0.31)\times10^{2}$	$(-2.87 \pm 0.33)\times10^{3}$
a_1	$(6.35 \pm 0.21)\times10^{-1}$	$(1.90 \pm 0.15)\times10^{0}$	$(-1.89 \pm 0.14)\times10^{0}$	$(7.84 \pm 0.73)\times10^{0}$
a_2	$(4.55 \pm 0.36)\times10^{-1}$	$(9.91 \pm 0.91)\times10^{-1}$	$(-9.90 \pm 0.81)\times10^{-1}$	$(3.06 \pm 0.73)\times10^{1}$
a_{11}	-	$(-2.22 \pm 0.17)\times10^{-3}$	$(2.21 \pm 0.17)\times10^{-3}$	-
a_{22}	-	-	-	$(-9.01\pm 1.47)\times10^{-2}$
a_{12}	-	$(-2.54 \pm 0.21)\times10^{-3}$	$(2.54 \pm 0.21)\times10^{-3}$	$(5.20\pm 0.35)\times10^{-2}$
F_{reg}	2,300	2,726	2,726	303
SS_{reg}	13,680	1,146	1,146	647,330
SS_{error}	71.3	2.3	2.3	11,738
R^2	0.9940	0.9976	0.9976	0.9790

Table 2 displays the values of the estimates for parameters a_0, a_1, a_2, a_{11}…, including corresponding 95% probability confidence intervals. Also, some statistical information is included for the models proposed for ethane conversion, ethylene selectivity, CO_x selectivity along with STY of ethylene. Only statistically significant parameters have been accounted for.

Models are adequate to predict the cited responses on the basis of the determination coefficient (R^2) and the F-value, while other tests (e.g. residuals distribution) were not included for practical reasons.

For ethane conversion, parameters a_0, a_1 and a_2 were statistically significant indicating and confirming that pure interaction terms (a_{ij}) along with quadratic effects (a_{ii}) do not impact the model predictions. In other words, a linear model on both temperature and space-time suffices to describe ethane conversion. In the case of ethylene selectivity, CO_x selectivity and STY of ethylene, models suitable to describe these responses are clearly non-linear. For the selectivity to ethylene and CO_x, the information in Table 2 indicates that all parameters, except for a_{22}, were statistically significant, implying that the quadratic effect of space-time does not have influence on these responses. For STY of ethylene, in contrast, the term a_{11} was not statistically significant; therefore, the quadratic effect of temperature was negligible. All these results are in a good agreement with the information provided by the ANOVA results,*i. e.*, the analytical assessment of main effects and interactions as well as graphical analysis of interactions.

The models discussed in the previous paragraphs were used to construct 3D plots, i.e., surface responses, from which the variations of values such as ethane conversion, ethylene selectivity and STY to ethylene as a result of simultaneous changes of temperature and space-time are observed. Surface responses are also useful to identify regions of convenient operation. Figure 7 contains the 3D plots of ethane conversion and ethylene selectivity, while Figure 8 includes the corresponding ones for CO_x selectivity and STY of ethylene. The topography of the surface varies among responses; specifically, ethane conversion 3D plot corresponds to a hill side, while selectivity to ethylene and CO_x as well as STY of ethylene seems saddle surface responses.

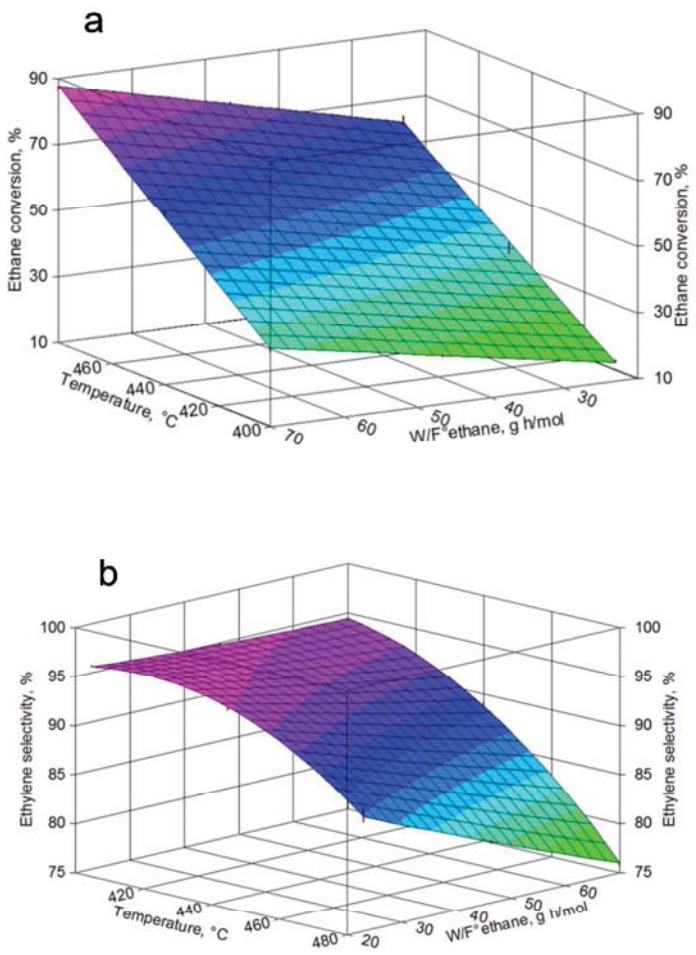

Figure 7. 3D response surfaces for (a) ethane conversion and (b) ethylene selectivity. Plots were constructed from the model fitted using the experimental design data. Varying temperature from 400 to 480 °C, space-time between 23 and 70 g_{cat} h (mol ethane)$^{-1}$ and an inlet molar ratio $C_2/O_2/N_2$ = 9/7/84.

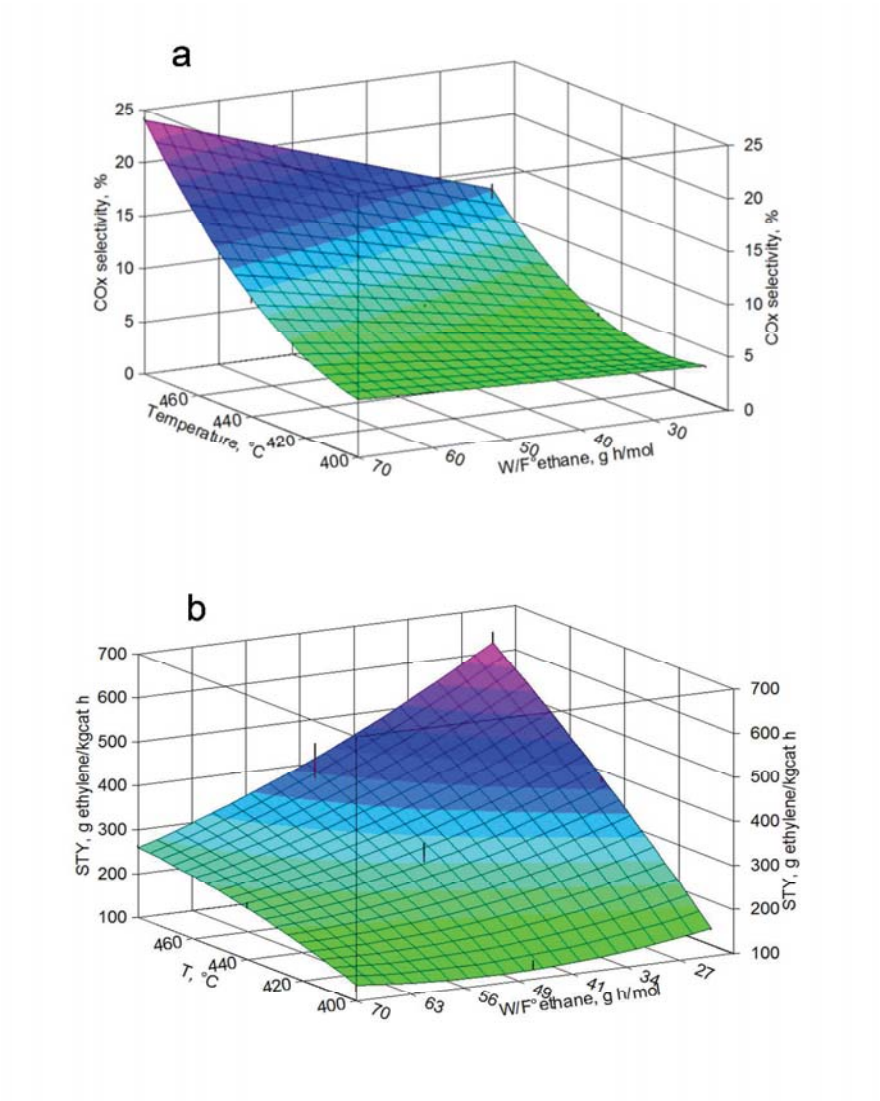

Figure 8. 3D response surfaces for (a) CO_x selectivity and (b) STY of ethylene. Plots were constructed from the model fitted using the experimental design data. Varying temperature from 400 to 480 °C, space-time between 23 and 70 g_{cat} h (mol ethane)$^{-1}$ and an inlet molar ratio $C_2/O_2/N_2$ = 9/7/84.

From a visual inspection of these graphs, the region of largest selectivity to ethylene (Figure 7b) requires operation at low temperature and space-time, whereas operating in the opposite direction clearly favors the formation of undesirable CO_x. Low temperature and space-time operation, however, lead to very low ethane conversions (Figure 7a). Besides, attractive

values of STY to ethylene (Figure 8b) are achieved when moving to high temperature and low space-time values.

3.4 Ethane and oxygen inlet partial pressure effect

Kinetic orders were computed by using the set of experiments where ethane and oxygen partial inlet pressure were varied. Figure 9 shows plots of the overall rate of ethane, ethylene, CO_2 and CO as a function of ethane and oxygen inlet partial pressure. It is observed that the overall production rate of the various species varies linearly with the inlet partial pressure of both ethane and oxygen. In all plots, however, the slope of the straight line resulting from varying the inlet partial pressure of ethane is greater than that resulting from adjusting the inlet partial pressure of oxygen. It is therefore clear that the overall production rate of the species mentioned above is more sensitive to changes in the inlet partial pressure of ethane compared with the inlet partial pressure of oxygen. As a consequence, the kinetic orders associated to the inlet partial pressure of oxygen are expected to exhibit lower absolute values.

Computed kinetic orders associated to the oxygen partial pressure are appreciably lower than 1.0, corresponding to 0.17, 0.36 and 0.43 for the overall rate of ethylene, CO_2 and CO, respectively. Kinetic orders related to ethane were, in contrast, systematically above 1.0 amounting to 1.46, 1.76 and 1.61 for the overall rates of ethylene, CO_2 and CO, respectively. These results indicate that, over the MoVTeNb mixed oxide catalyst, overall rates are substantially more dependent on the inlet partial pressure of hydrocarbon than on that of oxygen. In fact, the reaction of ethylene production is less sensitive to the oxygen partial pressure compared to the combustion reaction involved in CO_x formation. These results are, in the particular case of the kinetic orders related to oxygen, in a good agreement with previous reports.[23,24,26] For the corresponding overall rates, Kaddouri *et al.*[26] reported kinetic orders of 0.16, 0.17 and 0.25 for oxygen and 1.0, 1.14 and 1.35 for ethane, from lab-scale experiments over

a β-$NiMoO_4$ catalyst. Also, Lemonidou *et al.*[24] reported oxygen partial pressure reaction orders of 0.21 and 0.83 for the reactions of ethylene and CO_2 formation on a Ni-Nb based catalyst. For the same two reactions, Klose *et al.*[23] obtained values of 0.02 and 0.24 over a VO_x/γ-Al_2O_3 catalyst.

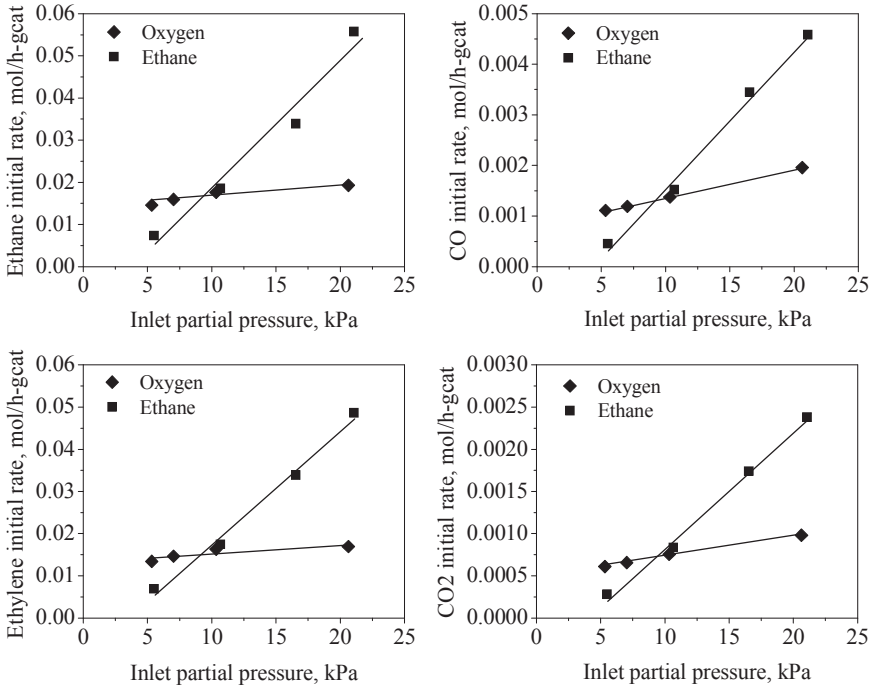

Figure 9. Overall rate of ethane, ethylene, CO_2 and CO as a function of the partial pressures of ethane and oxygen. $T_{reaction}$= 440 °C, ethane (or oxygen) inlet partial pressure ranged from 5.1 to 22.3 kPa, and space-time between 10 and 140 g_{cat} h (mol ethane)$^{-1}$.

3.5 Apparent kinetics: model parameters and performance

Table 3 shows reparameterized pre-exponential factors, activation energies and reaction orders, including the corresponding 95% probability confidence intervals, obtained by regression for the power-law kinetic model. Notice that the parameters for the oxidation of ethylene to CO_2 according to the reaction network of Scheme 1, are not reported, as the corresponding activation energy could not be estimated with statistical significance. This indicates that CO_2 is most likely formed from ethane, and CO is produced from both ethane and ethylene. Reaction orders were estimated using the values of kinetic orders reported in section 3.4 as initial estimations. Initial

values of the reaction orders associated to secondary reactions of CO_x formation from ethylene were obtained via regression of $\ln(R^o_{COx})$ vs. $\ln(P^o_{02})$ as well as $\ln(R^o_{COx})$ vs. $\ln(P_{ethylene})$ experimental data, following a methodology similar to that described earlier.

Table 3. Non-isothermal parameters results containing reparameterized pre-exponential factors and activation energies with corresponding 95% probability confidence. Reaction orders are also included.

Reaction	A_{rep}, $mol(g_{cat}\cdot h\cdot kPa^{\alpha+\beta})^{-1}$		E, $kJ(mol)^{-1}$		α	β
$C_2H_6+0.5O_2\rightarrow C_2H_4+H_2O$	5.34×10^{-4}	$\pm 2.97\times10^{-5}$	119	± 12.6	1.50	0.13
$C_2H_6+3.5O_2\rightarrow 2CO_2+3H_2O$	7.44×10^{-6}	$\pm1.24\times10^{-6}$	217	±33.1	1.78	0.36
$C_2H_6+2.5O_2\rightarrow 2CO+3H_2O$	1.37×10^{-5}	$\pm1.53\times10^{-6}$	143	± 53.2	1.80	0.24
$C_2H_4+2O_2\rightarrow 2CO_2+2H_2O$		-		n. r.	-	-
$C_2H_4+2O_2\rightarrow 2CO+2H_2O$	3.38×10^{-5}	$\pm3.95\times10^{-6}$	242	±37.8	1.33	0.30

F_{reg}= 542.9, F_{tab}= 2.79, t_{tab}=1.97 at 1-alpha = 0.95 and 244 degrees of freedom

n.r. : not reported as parameters were not statistically significant

It is observed in Table 3 that the reaction responsible for the formation of ethylene exhibited the lowest activation energy with a value of 119 kJ $(mol)^{-1}$. The reoxidation of ethylene into CO is, in contrast, the reaction that demands the largest amount of energy to proceed with an activation energy equal to 242 kJ $(mol)^{-1}$. Over the catalyst investigated in this work, reactions involving the formation of CO_x species require more energy than the desired reaction leading to the formation of ethylene. Among the oxidation reactions considered in the kinetic model, the one that demands the lowest amount of energy is the oxidation of ethane to CO with activation energy of 143 $kJmol^{-1}$. Additionally, the fact that oxidation reactions exhibit a larger activation

energy compared with the partial oxidation (i.e., ethylene formation) indicates that an increased temperature favors oxidation reactions to produce CO_x.

On the basis of the information included in Table 3, the values of reparameterized pre-exponential factor, $A_{rep,i}$, which actually corresponds to the rate coefficient of reaction i computed at T_m, evolve as follows: ethylene > CO from ethylene > CO from ethane > CO_2 from ethane. At T_m, $A_{rep,i}$ for ethylene production is three orders or magnitude larger than that of the formation of CO_2 out of ethane. This trend is qualitatively in agreement with the results discussed in previous section.

The main value of pre-exponential factors (A) in $mol(g_{cat}h\ kPa^{\alpha+\beta})^{-1}$ were calculated from reparameterized pre-exponential factors included in Table 3 for a mean temperature (T_m) equal to 440 °C. Thus, for the four reactions with statistically significant parameter values of A amounted to 2.8×10^5, 6.2×10^{10}, 3.9×10^5 and 1.7×10^{13} $mol(g_{cat}hkPa^{\alpha+\beta})^{-1}$, respectively. Notice that the pre-exponential factor of the first reaction is eight orders of magnitude smaller than the one of fourth reaction. In general, it is observed that values of pre-exponential factors evolve in an opposite direction compared with activation energies, as the reaction with the highest value of activation energy (242 $kJmol^{-1}$ for CO formation from ethylene) exhibited the largest pre-exponential factor. It is clear that the differences in the magnitude orders of pre-exponential factors compensate detected deviations in the values of activation energies.

Corresponding main values of reaction orders for the four reactions with statistically significant parameters in accordance with Table 3 were 1.50, 1.78, 1.80 and 1.33 for the partial pressure of hydrocarbons, and 0.13, 0.36, 0.24 and 0.30 for the partial pressure of oxygen. Evidently, all the reaction rates composing the kinetic model exhibit very low dependence to the oxygen partial pressure, contrary to what occurs with the partial pressure of hydrocarbons. As

mentioned before, the effect observed for the oxygen concentration is in agreement with information outlined in other publications.[23,24]

F-test was used to verify the model adequacy and the global significance of the regression. Table 3 reports a value of F_{reg} equal to 460; F_{tab} amounted to 2.79 for 244 degrees of freedom and 95% probability.

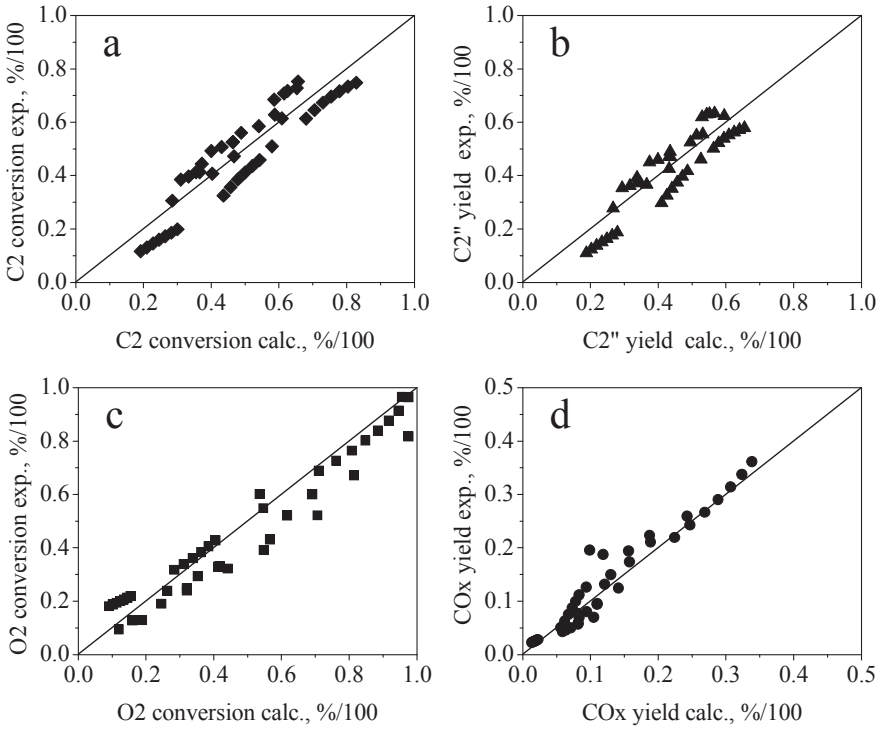

Figure 10. Parity plots showing calculated versus experimental conversions (ethane and oxygen) and products (ethylene and CO_x) yield. Conversions and yields were computed with a power-law kinetic model.

Finally, the parity diagrams were constructed in order to compare experimental data versus corresponding data predicted by the kinetic model. Figures 10a-b compare experimental versus predicted ethane and oxygen conversions, while Figures 10c-d contrast experimental versus predicted ethylene and CO_x molar yields. It is noted that model predictions for both reactants

conversion and product yields describe very well the kinetic phenomena occurring on MoVTeNb mixed oxide catalyst.

4 Conclusions

In this work, the effects of temperature (T) and space-time (W) were investigated on the catalytic performance of a MoVTeNb mixed oxide catalyst for the ODH of ethane, by means of a set experiments included in a 3^k experimental design. Linear main effects of T and W on ethane conversion were observed without detecting interaction between these two factors. In contrast, main effect of T and W are not linear on the selectivity to ethylene or CO_x, while an interaction between T and W is observed. Ethane conversion is clearly enhanced at high values of both T and W, although, under these conditions, CO_x production rises in detriment of ethylene formation. Operation at high temperature and low space-time is convenient for obtaining high values of space time yield of ethylene, a key parameter from the industrial point of view.

Experiments varying ethane and oxygen inlet partial pressure indicated a very low dependency of the overall rate formation of the various product species, in particular that leading to ethylene, on the inlet partial pressure of oxygen with experimental kinetic orders within the 0.17 – 0.43 range.

Kinetic modeling indicates that CO_2 is mainly formed from ethane while CO is produced from both ethane and ethylene, and exhibits low values of reaction orders associated to the partial pressure of oxygen. Kinetic information also indicates that the formation of ethylene is the reaction with the lowest demand of energy (119 $kJmol^{-1}$), while the ethylene oxidation into CO is the reaction that requires the highest amount of energy (242 $kJmol^{-1}$). Pre-exponential factors of the most energy demanding reaction are, in general, several orders of magnitude higher than

those of the other reactions, thus partially compensating the existing differences in values of activation energies.

Acknowledgments

This work was financially supported by the Instituto Mexicano del Petroleo. Technical support from Eng. G. Alonso-Ramirez is gratefully acknowledged.

Supporting Information

The main physicochemical properties of the material and ANOVA results for ethylene selectivity, CO_x selectivity and STY of ethylene are presented in Supporting Information. This material is available free of charge via the Internet at http://pubs.acs.org.

References

(1) Lippe, D. Ethylene markets return to normal. *Oil & Gas Journal* **2011**, *109-10*, 94.

(2) Bhasin, M. M. Is true ethane oxydehydrogenation feasible? *Top. Catal.* **2003**, *23, 1-4*, 145.

(3) Sanfilippo, D.; Miracca, I. Dehydrogenation of paraffins: synergies between catalyst design and reactor engineering. *Catal. Today* **2006**, *111, 1-2,* 133.

(4) Grabowski, R. Kinetics of oxidative dehydrogenation of C_2-C_3 alkanes on oxide catalysts. *Catal. Rev.* **2006**, *48-2*, 199.

(5) Cavani, F.; Ballarini N.; Cercola A. Oxidative dehydrogenation of ethane and propane: How far from commercial implementation? *Catal. Today* **2007**, *127*, 113.

(6) Bhasin, M. M.; McCain, J. H.; Vora, B. V.; Imai, T.; Pujado, P. R. Dehydrogenation and oxydehydrogenation of paraffins to olefins. *Appl. Catal. A: Gen.* **2001**, *221*, 397.

(7) Lange, J. P.; Schoonebeek, R. J.; Mercera, P. D. L.; van Breukelen F. W. Oxycracking of hydrocarbons: chemistry, technology and economic potential. *Appl. Catal. A: Gen.* **2005**, *283*, 243.

(8) Ruth, K.; Kieffer, R.; Burch R. Mo-V-Nb Oxide catalyst for the partial oxidation of ethane. *J. Catal.* **1998**, *175*, 16.

(9) Hatano, M.; Kayo, A.; US 5,049,692 (**1991**), assigned to Mitsubishi Kasei Co.

(10) Lopez Nieto, J. M.; Botella, P.; Vázquez, M. I.;Dejoz, A. The selective oxidative dehydrogenation of ethane over hydrothermally synthesised MoVTeNb catalysts. *Chem. Commun.* **2002**, 1906.

(11) Lopez Nieto, J. M.; Botella, P.; Vázquez, M. I.;Dejoz, A. WO 03/064035 A1 (**2003**) assigned to CSIC-UPV.

(12) Lopez Nieto, J. M.; Botella, P.; Vázquez, M. I.;Dejoz, A.US 7,319,179 B2 (**2008**) assigned to CSIC-UPV.

(13) Solsona, B.; Vázquez, M.I.; Ivars, F.; Dejoz, A.; Concepción, P.; Lopez Nieto, J. M.; Selective oxidation of propane and ethane on diluted Mo–V–Nb–Te mixed-oxide catalysts. *J. Catal.* **2007**, *252*, 271.

(14) Xie, Q.; Chen L.; Weng, W., Wan, H. Preparation of MoVTe(Sb)Nb mixed oxide catalysts using a slurry method for selective dehydrogenation of ethane. *J. Mol. Catal. A: Chem.* **2005**, *240*, 191.

(15) Deniau, B.; Millet, J .M .M .; Loridanta, S.; Christin, N.; Dubois, J.L. Effect of several cationic substitutions in the *M1* active phase of the MoVTeNbO catalysts used for the oxidation of propane to acrylic acid. *J. Catal.* **2008**, *260*, 30.

(16) DeSanto, P.; Buttrey, D.J.; Grasselli, R.K.; Lugmair, C.G.; Volpe, A.F.; Toby, B.H. Structural characterization of the orthorhombic phase M1 in MoVNbTeO propane ammoxidation catalyst. *Top. Catal.* **2003**, *23*, 23.

(17) Aouine, M., Dubois, J.L.; Millet, J.M.M. Crystal chemistry and phase composition of the MoVTeNbO catalysts for the ammoxidation of propane.*Chem. Commun.* **2001**, 1180.

(18) Botella, P.; García-González, E.; Lopez Nieto, J.M.; González-Calbet, J.M. MoVTeNbO multifunctional catalysts: Correlation between constituent crystalline phases and catalytic performance. *Sol. St. Sci.* **2005**, *7*, 507.

(19) Millet, J. M. M.; Baca, M.; Pigamo, A.; Vitry, D.; Ueda, W; Dubois, J.L. Study of the valence state and coordination of antimony in MoVSbO catalysts determined by XANES and EXAFS, *Appl. Catal. A: Gen.* **2003**, *244*, 359.

(20) Deniau, B.; Bergeret, G.; Jouguet,B.; Dubois, J. L.; Millet, J. M. M. Preparation of Single M1 Phase MoVTe(Sb)NbO Catalyst: Study of the Effect of M2 Phase Dissolution on the Structure and Catalytic Properties. *Top Catal.* **2008**, *50*, 33.

(21) Klose, F.; Wolf, T.; Thomas, S.; Seidel-Morgenstern, A. Operation modes of packed-bed membrane reactions in the catalytic oxidation of hydrocarbons. *Appl. Catal. A: Gen.* **2004**, *257*, 193.

(22) Skoufa, S.; Heracleous, E., Lemonidou, A. A. Investigation of engineering aspects in ethane ODH over highly selective $Ni_{0.85}Nb_{0.16}O_x$ catalyst. *Chem. Eng. Sci.* **2012**, *84*, 48.

(23) Klose, F.; Joshi, M.; Hamel, C.; Seidel-Morgenstern, A. Selective oxidation of ethane over a VO_x/γ-Al_2O_3 catalyst – investigation of the reaction network. *Appl. Catal. A: Gen.* **2004**, *26*, 101.

(24) Lemonidou, A. A.; Heracleous, E. Ni-Nb-O mixed oxides as highly active and selective catalyst for ethane production via ethane oxidative dehydrogenation. Part II: Mechanistic aspects and kinetic modeling. *J. Catal.* **2006**, *237*, 175.

(25) Gaab, S.; Find, J.; Müller, T. E.; Lercher, J. A. Kinetics and mechanism of the oxidative dehydrogenation of ethane over Li/Dy/Mg/O/(Cl) mixed oxide catalysts. *Top. Catal.* **2007**, *46, 1-2*, 101.

(26) Kaddouri, A.; Anouchinsky, R.; Mazzocchia, C.; Madeira, L. M.; Portela, M. F. Oxidative dehydrogenation of ethane on the α and β phases of $NiMoO_4$. *Catal. Today* **1998**, *40, 2-3*, 201.

(27) Malleswara-Rao, T. V.; Deo, G. Steady state kinetic parameters of bulk V_2O_5 for ethane and propane oxidation reactions. *Catal. Comm.* **2007**, *8*, 957.

(28) Iglesia, E.; Argyle, M. D.; Chen, K.; Bell, A. T. Ethane oxidative dehydrogenation pathways on vanadium oxide catalysts. *J. Phys. Chem. B* **2002**, *106*, 5421.

(29) Grabowski, R.; Sloczynski, J. Kinetics of oxidative dehydrogenation of propane and ethane on VOx/SiO_2 pure and with potassium additive. *Chem. Eng. Proc.* **2005**, *44*, 1082.

(30) Mears, D. E. Test for transport limitations in experimental catalytic reactors. *Ind. Eng. Chem. Proc. Des. Dev.* **1997**, *10*, 541.

(31) Pérez-Ramírez, J.; Berger, R. J.; Mul, G.; Kapteijin, F.; Moulijin, J. A. The six flow reactor technology: A review of fast catalyst screening and kinetic studies. *Catal. Today* **2000**, *60*, 93.

(32) Petzold L. R.; Hindmarsh, C., solver for ODE equations. http://www.netlib.com, **1997**.

(33) Boggs, P. T.; Byrd, R. H.; Rogers J. E.; Schnabel. R. B. ODRPACK 2.01 solver. http://www.netlib.com, **2009**.